Available online at www.sciencedirect.com

ScienceDirect

Journal of Solid State Chemistry 180 (2007) 785–791

JOURNAL OF SOLID STATE CHEMISTRY

www.elsevier.com/locate/jssc

The structure and ordering of zirconium and hafnium containing garnets studied by electron channelling, neutron diffraction and Mössbauer spectroscopy

Karl R. Whittle[a,f,*], Gregory R. Lumpkin[a,c], Frank J. Berry[b], Gordon Oates[b], Katherine L. Smith[c], Sergey Yudintsev[d], Nestor J. Zaluzec[e]

[a]*Department of Earth Sciences, Downing Street, Cambridge, CB2 3EQ, UK*
[b]*Department of Chemistry, The Open University, Walton Hall, Milton Keynes, MK7 6AA, UK*
[c]*Materials Division, Australian Nuclear Science and Technology Organisation, Private Mail Bag 1, Menai, NSW 2234, Australia*
[d]*Institute of Geology of Ore Deposits, Russian Academy of Sciences (RAS), Staromonetnii Pereulok 35, Moscow 109017, Russian Federation*
[e]*Materials Science Division, Argonne National Laboratory, 9700 South Cass Avenue, Argonne, IL 60439, USA*
[f]*Department of Engineering Materials, University of Sheffield, Sir Robert Hadfield Building, Mappin Street, Sheffield, S1 3JD, UK*

Received 5 September 2006; received in revised form 25 November 2006; accepted 4 December 2006
Available online 15 December 2006

Abstract

Garnets, $A_3B_2C_3O_{12}$, are an important group of minerals and have potential uses in the safe immobilisation of high-level nuclear waste. They have been found naturally to incorporate Zr, Ti and Fe, three elements of interest in the safe storage of nuclear waste. Kimzeyite, $Ca_3(Zr,Ti)_2(Si,Al,Fe)_3O_{12}$, is a naturally occurring garnet that contains Zr in a high percentage~30 wt%. For such a material to be of potential immobilisation for nuclear waste the structure needs to be completely understood. Electron channelling studies have shown that the Zr/Ti cations are located on the *Y*-site, with the Al/Fe cations located on the *Z*-site. This work has investigated synthetic analogues of kimzeyite, $Ca_3(Zr,Hf)_2(Al,Fe,Si)_3O_{12}$, by neutron powder diffraction, using the C2 spectrometer at the Chalk River nuclear facility, coupled with ^{57}Fe Mössbauer spectroscopy. Such work has allowed the structure of the synthetic material to be determined along with the distribution of cations across the X (CN = 8), Y (CN = 6), and Z (CN = 4) sites. Results have shown that it is possible to synthesise $Ca_3(Zr,Hf)_2(Al,Fe,Si)_3O_{12}$ with a range of Al/Fe ratios containing Zr and Hf. The Mössbauer data has indicated the Fe is located on the Z site. The structural analyses show that the unit cell changes linearly as a function of composition, and analysis of the disorder indicates that the Zr, Hf reside on the Y site and the Al, Fe, and Si reside on the Z site.

Keywords: Mössbauer; Garnet; Kimzeyite; Electron channelling

1. Introduction

Garnet, of general composition $A_3B_2C_3O_{12}$, is a widely found structure type in nature. The majority of garnets are based on silicates, e.g., grossular ($Ca_3Al_2Si_3O_{12}$) [1]. The garnet structure-type is cubic with $Ia3d$ symmetry with the sites listed below:

(i) X cations–cubic (distorted) co-ordinated on special position 24*c* (3/8, 0, 1/4), e.g., Y^{3+}, Ca^{2+}, Mn^{2+}, Mg^{2+} and Fe^{2+}.
(ii) Y cations–octahedrally co-ordinated on special position 16*a* (0, 0, 0), e.g., Fe^{3+}, Al^{3+}, Cr^{3+} and Ti^{4+}.
(iii) Z cations–tetrahedrally co-ordinated on special position 24*d* (1/8, 0,1/4), e.g., Si^{4+}, Ge^{4+}, Fe^{3+} and Al^{4+}.
(iv) Anions–tetrahedrally co-ordinated on general position 96*h* (x, y, z).

---

*Corresponding author. Fax: +44 114 222 5943.
E-mail address: k.r.whittle@shef.ac.uk (K.R. Whittle).

0022-4596/$ - see front matter © 2006 Elsevier Inc. All rights reserved.
doi:10.1016/j.jssc.2006.12.006

Topologically, the garnet structure can be described as a framework of corner sharing *Y* octahedra and *Z* tetrahedra which alternate to form chains in the ⟨100⟩ directions. These chains are cross linked via the *Y* octahedron located at the body centred lattice point 1/2, 1/2, 1/2 to form a three dimensional framework. However, the *X* dodecahedra and *Z* tetrahedra also form a three dimensional framework via edge sharing, with discreet chains of alternating *A* and *C* cations along ⟨100⟩ directions, connected by edge sharing *X* dodecahedra. An illustrative unit-cell showing the arrangement of polyhedra is shown in Fig. 1.

Naturally occurring garnets are found with a large range of elemental compositions with the cations located across more than one site in the lattice, e.g., schorlomite, a naturally occurring garnet containing Ti^{4+} has the formulation $(Ca_{2.87}Mg_{0.10}Na_{0.04})(Ti_{1.06}Fe_{0.69}Al_{0.14}Zr_{0.04}Mg_{0.04}Mn_{0.03}V_{0.01})(Si_{2.35}Fe_{0.65})O_{12}$ has Fe and Mg located on multiple sites. Garnets can be prepared containing U, Th and lanthanide elements; as such they make ideal candidates for the long-term storage of actinide waste.

Current research in new materials for actinide waste tend to contain titanium and zirconium, this was originally due to the existence of compatible Ti phases for high-level waste, e.g., hollandite, pyrochlore and zirconolite. Zirconium has been added in recent research to enhance the stability to radiation damage. In nature there are two garnets which make ideal candidates for wasteform research which have high levels of Ti^{4+} (schorlomite) or Zr^{4+} (kimzeyite), with kimzeyite and simplified analogues being the focus of this work.

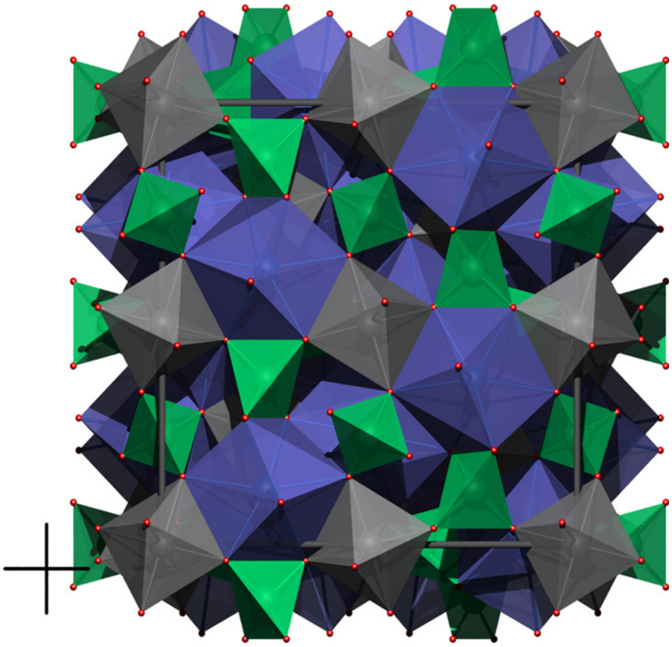

Fig. 1. Diagrammatic representation of the garnet structure, the view is aligned on the 1 0 0 face. The blue polyhedra are the *A*-site 8 co-ordinated cations, the grey octahedra are the *B*-site cations, and the green tetrahedra are the *C*-site cations. The red spheres indicate the location of the oxygen anions.

Kimzeyite $Ca_3(Zr,Ti)_2(Si,Al,Fe)_3O_{12}$ [2–5] was originally reported in 1961 for a sample from Magnet Cove in Arkansas, it is a naturally occurring garnet that contains high levels of Zr (~30 wt% ZrO_2). There have been two subsequent analyses published based on samples from the Aeolian Islands, and the Sabatini Volcanic district, both in Italy. All three analyses give similar values for elemental composition and crystal parameters.

As these garnets are naturally occurring with good long term stability, they are ideal to study as potential storage media for radioactive nuclear waste. In addition to making samples close to the ideal kimzeyite composition, compositions with a simpler elemental distribution and containing Hf and a variable Al/Fe ratio are examined in this study. We have used neutron diffraction and Mössbauer spectroscopy in combination such that the Fe cations are located by Mössbauer spectroscopy, and then used in the refinement of the structure, thus allowing the oxygen position to be determined accurately. If the location of the Fe could not be determined independently, there would always be some doubt about the location of the Fe within the lattice, particularly as in some garnets Fe is found on the octahedral site, e.g., yttrium iron garnet. In order to understand the long term stability of these materials to hydrothermal alteration the definite cation location is beneficial. In addition to synthetic samples, we determine the cation distribution in a sample of kimzeyite from Magnet Cove using electron channelling techniques.

2. Experimental

Stoichiometric mixtures of $CaCO_3$ (Alfa-Aesar, 99.9%), SiO_2 (Aldrich, 99.9%), Al_2O_3 (Aldrich, 99.9%), Fe_2O_3 (Aldrich, 99.9%), ZrO_2 (Alfa-Aesar, 99.5%) and HfO_2 (Alfa-Aesar, 99.5%), were ground together in an agate ball-mill for 60 min. The samples were dried and heated as pellets for 24 h at 850 °C to decarbonate the $CaCO_3$ in situ. After heating the samples were ground and calcined as pellets at 1400 °C for 48 h, placed on α-Al_2O_3 plates. After cooling, the samples were ground to a fine powder sufficient to pass through a 38 μm sieve. Once ground the phase purity was checked using laboratory X-ray powder diffraction.

$Ca_3Zr_2Fe_2SiO_{12}$, $Ca_3Zr_2Fe_{1.5}Al_{0.5}SiO_{12}$ and $Ca_3Zr_2FeAlSiO_{12}$ were checked for purity using a JEOL 6400 SEM operating at 15 kV. Microanalyses were obtained using a Noran Voyager energy dispersive spectrometer (EDX) attached to this microscope. The instrument was operated in standardless mode; however, the sensitivity factors were calibrated for semi-quantitative analysis using a range of synthetic and natural standard materials. Spectra were usually acquired for 500 s and reduced to weight percent oxides using a digital top hat filter to suppress the background, a library of reference spectra for multiple least squares peak fitting and full matrix (ZAF) corrections.

Samples based on the compositions $Ca_3Hf_2Fe_2SiO_{12}$ and $Ca_3Hf_2FeAlSiO_{12}$ were analysed using TEM/ EDX. TEM samples were prepared by crushing small fragments in methanol and collecting the suspension on holey carbon coated copper grids. Samples were analysed using a JEOL 2000FXII TEM operated at 200 kV and calibrated for selected area diffraction over a range of objective lens currents using a gold film standard. The compositions of the grains were checked by EDX analysis using a Link ISIS energy dispersive spectrometer attached to the TEM. The *k*-factors required for the quantitative thin film analyses were determined from a range of synthetic and natural standard materials. Spectra were usually acquired for 600 s and processed using a digital top hat filter to suppress the background, a library of reference spectra for multiple least squares peak fitting, and a Cliff-Lorimer ratio procedure to reduce the data to weight percent oxides (details are given in Lumpkin et al. [6]).

The kimzeyite sample is from the Kimzey quarry, Magnet Cove, Arkansas and was provided by Robert G. Middleton, Philadelphia Academy of Natural Sciences, sample number 18635. For the electron channelling experiments on kimzeyite we used the [311] zone axis as the starting point. Independent measurements of a grossular garnet sample have shown that this crystallographic orientation is sensitive to the distribution of elements across the *B* and *C* sites. Since the *A* site is nearly filled by Ca and only a small amount of Mg is present (see results below), we have ignored this site in our analysis of the data. We acquired a data set for multivariate analysis by collecting 25 EDX spectra at successive tilt angles of approximately 0.1 degrees away from the exact zone axis condition. The measured intensities of the Al*K*, Si*K*, Ti*K*, Fe*K*, Zr*K*, and Nb*K* X-ray lines were then used in a multiple regression analysis in which Zr and Si were treated as the dependent variables (e.g., the host atoms for the *Y* and *Z* sites, respectively) and Al, Fe, Ti, and Nb were treated as independent variables (unknown impurity atom distribution over *Y* and *Z*). The analysis was conducted following previously established procedures [7,8].

Mössbauer spectra, collected on the Zr containing samples, were recorded at 298 K with a microprocessor controlled spectrometer using a ca 25 μCi ^{57}Co/Rh source. All spectra were computer fitted and the chemical isomer shift data are quoted relative to that of metallic iron at 298 K.

Constant wavelength neutron diffraction patterns were collected, at room temperature, for all samples using the C2-DualSpec diffractometer at the Chalk River National Laboratory, Canada, operating at an incident wavelength of 1.3300 Å (determined using an Al_2O_3 standard). Sample diffraction patterns were collected over the angular range 5–115° 2θ, with an angular resolution of 0.1°, corresponding to a *d*-spacing range of ~0.8–15.26 Å. The data were analysed by Rietveld refinement using GSAS [9] with the EXPGUI toolkit [10], with the composition used based on those obtained by electron microanalaysis. The set of instrumental and structural parameters refined were the overall scale factor, unit cell dimensions, a Chebyschev polynomial background function, the widths of the Gaussian and Lorenztian components of a Voigt function describing the reflection line shape, determined using a Le-Bail fit, and the O(*96h*) positional parameters. The thermal parameters were refined isotropically with the overall absorption of the sample calculated, using standard techniques, to ensure the moderately high absorption of Hf, ~100 barns, was accounted for.

3. Results and discussion

3.1. Electron microanalysis

The elemental analysis (Table 1) shows that the samples prepared are in good agreement with the expected stoichiometric composition. Small discrepancies are probably due to small inaccuracies in both the composition of the initial mix and possible small sensitivity problems with the electron microanalysis.

3.2. Electron channelling

The composition, $(Ca_{2.94}Mg_{0.05})(Zr_{1.72}Ti_{0.26}Nb_{0.09})(Fe_{1.09}Si_{0.94}Al_{0.87})O_{12}$, of the kimzeyite crystal used in this study was determined from the average of 10 non-channelling EDX spectra and is similar to previously published chemical data [3]. The difference in our EDX analysis and the chemical analysis reported by Milton et al. [3] are mostly likely due to the presence of numerous inclusions (e.g., perovskite and aluminosilicate minerals) in the garnets from this locality. These inclusions would largely explain the higher Ca, Ti, and Al contents derived from the chemical analysis. We avoided these inclusions in our EDX microanalyses. The difference between our analysis and those reported on kimzeyite crystals from other localities [4,5], is mostly likely due to the differences in bulk composition between the different and rather exotic rock types; e.g., intrusive carbonatite (Magnet Cove) vs shoshonitic basalt (Stromboli) vs pyroclastic flows (Anguillara). Additional potential problems with the natural samples is variation in composition from place to place within the host rocks (different rock units) and chemical zoning within the crystals themselves due to changes in composition of the system with time during crystallisation. The electron channelling results are summarised in Table 2, where we give the regression coefficients and errors for each "impurity" atom versus the two host atoms. All four of the individual models appear to be robust, as indicated by the statistical parameters R^2 (generally >0.99) and *F*. The coefficients are then converted to atomic concentrations per formula unit by knowing the total number of atoms for each site ($Y = 2$, $Z = 3$) and the atomic *k*-factors for each element. The latter were calculated from the mass-based experimental *k*-factors and are listed in Table 2. The values of n-cih presented in Table 2 are 2 minus the summed occupancies on the Zr-site, and 3 minus the summed occupancies of the Si site. This value is a validity check on the results when compared with

Table 1
Average elemental analysis of samples using SEM and TEM based techniques, the compositions have been normalised to 12 oxygens. The values are shown in formula units with the standard deviation

Element	$Ca_3Zr_2FeAlSiO_{12}$		$Ca_3Zr_2Fe_{1.5}Al_{0.5}SiO_{12}$		$Ca_3Zr_2Fe_2SiO_{12}$	
Ca	3.222	0.038	3.063	0.045	3.189	0.041
Zr	2.038	0.023	2.039	0.026	2.024	0.024
Al	1.053	0.026	0.486	0.019	0.009	0.011
Fe	0.917	0.043	1.440	0.058	1.938	0.058
Si	0.929	0.033	0.801	0.025	0.920	0.024
O	12.000		12.000		12.000	

Element	$Ca_3Hf_2FeAlSiO_{12}$		$Ca_3Hf_2Fe_2SiO_{12}$	
Ca	3.054	0.17	2.960	0.17
Hf	1.808	0.18	1.902	0.18
Zr	0.016	0.01	0.015	0.01
Al	1.217	0.11	0.006	0.11
Fe	0.979	0.04	2.155	0.04
Si	0.995	0.06	0.983	0.12
O	12.00		12.00	

Table 2
Parameters used in the electron channelling analysis of kimzeyite along with the results obtained. R^2, SD, and F are the classically used means of testing a model in statistical analysis. Nb*K* refers the *K*-edge X-rays of Nb used in the analysis

Alpha coefficient

Element	Zr*K*	Error	Si	Error	R^2	SD	*F*
Ti	0.186	0.004	0.088	0.009	0.9996	155	24997
Al	−0.016	0.005	0.761	0.012	0.9997	210	30473
Fe	0.010	0.010	1.509	0.023	0.9997	408	35670
Nb*K*	0.048	0.002	0.006	0.004	0.9983	75	5487

k-factor matrix	Zr*K*	Si
Ti	0.61	0.76
Al	0.96	1.20
Fe	0.56	0.70
Nb*K*	0.99	1.24

Site occupancy calculation	Zr*K*	Error	Si	Error	Total	Error
Ti	0.197	0.005	0.066	0.019	0.263	0.008
Al	−0.027	0.009	0.9	0.027	0.873	0.027
Fe	0.010	0.011	1.041	0.030	1.051	0.029
Nb*K*	0.082	0.004	0.008	0.009	0.090	0.004
n-cih	1.738		0.985			

an average composition determined from non-channelling measurements. Results of these calculations indicate that about 75% of the Ti and essentially the Nb resides on the octahedral *Y* site with Zr; whereas, all of the Al and Fe are located on the *Z* site. The total concentrations of these atoms, plus those of the host atoms (determined by difference), are in excellent agreement with the composition of the crystal as determined from non-channelling EDX spectra. The diffraction pattern for the 3 1 1 zone axis chosen in these measurements and a bright-field image of the crystal are shown in Fig. 2.

3.3. Mössbauer spectroscopy

The numeric results from the fitting of the data are shown in Table 3, with an illustrative fit shown in Fig. 3. The data was best described when fitted to a single quadrupole split absorption (doublet). This doublet is best associated with the tetrahedrally co-ordinated Fe^{3+} and agrees with other synthetic and naturally occurring Fe containing garnets, illustrative values shown in Table 4. Since the sample contained only a single paramagnetic doublet it indicates that there is no magnetic ordering

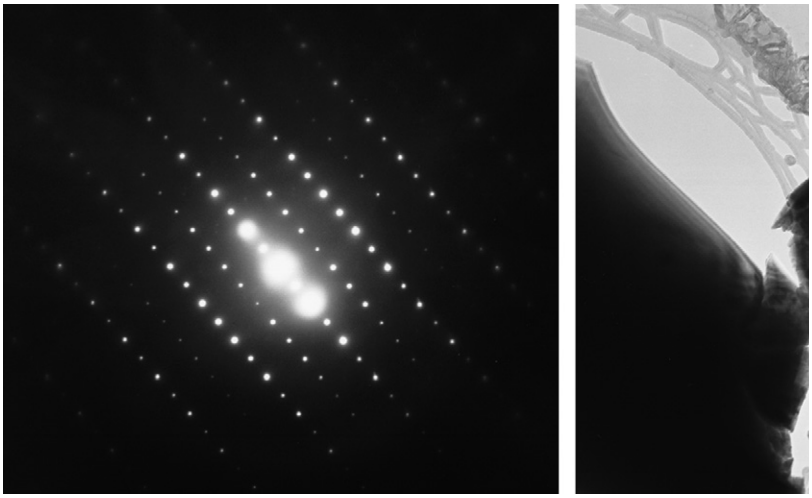

Fig. 2. Dynamical diffraction pattern for kimzeyite along the 3 1 1 direction, used in the electron channelling analysis, and a bright field image of the sample investigated, the magnification is 25 000.

Table 3
Results from analysis of collected ^{57}Fe Mössbauer spectra

System	Isomer shift (mm s^{-1})	Quadrupole split (mm s^{-1})
$Ca_3Zr_2FeAlSiO_{12}$	0.19	1.10
$Ca_3Zr_2Fe_{1.5}Al_{0.5}SiO_{12}$	0.18	1.05
$Ca_3Zr_2Fe_2SiO_{12}$	0.18	1.03

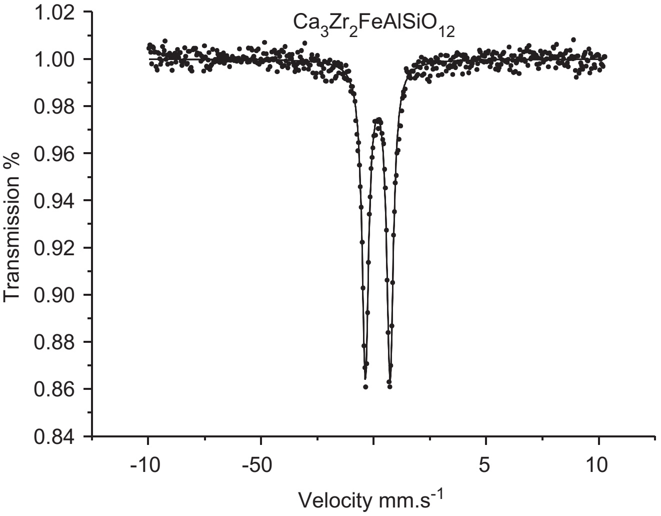

Fig. 3. Results obtained from analysis of ^{57}Fe Mössbauer data on $Ca_3Zr_2FeAlSiO_{12}$, the velocity scale is relative to an α-Fe foil, collected at 298 K.

associated with these garnets at the temperature of measurement i.e., 298 K. If there was magnetic ordering then a sextet would be expected, e.g., $Y_3Fe_5O_{12}$ shows two sextets due to the *Y* and *Z* sites being magnetically ordered. The paramagnetism in these samples indicate there is no ordering of cations on the *Z*-site, such an order would give rise to a super/modulated structure in the electron and neutron diffraction studies and none was observed.

When the results are compared with values previously recorded for natural kimzeyite and related garnets [11–14] very good agreement is found for the tetrahedral site, with no visible contribution from the octahedral site. This is particular apparent in the values reported for $YCa_2Zr_2Fe_2AlO_{12}$ [11], a similar composition, where the Fe^{3+} was reported to be located on the tetrahedral site. Small disagreements in the compared values are probably down to the elemental compositions of the garnets e.g., natural Kimzeyite contains elements known to prefer tetrahedral co-ordination e.g., Al^{3+}, Si^{4+}, if these preferentially fill the *Z*-site then the remaining Fe^{3+} will start to occupy the octahedral *B*-site.

3.4. Neutron diffraction

The Rietveld analyses were based on the compositions determined by the elemental electron microanalysis. The exact compositions were slightly simplified as in the majority of cases the samples were within two standard deviations of the compositions desired. The results from the refinements are shown in Table 5, with an illustrative fit shown in Fig. 4. All fits converged to give $wR_p \sim 0.05$. The unit cell values were found to closely match those for both natural Kimzeyite [3–5] and other garnets containing Fe, particularly the values previously reported for $Ca_3Zr_2Fe_2SiO_{12}$ [15]. Using the information provided by the Mössbauer spectroscopy a model was chosen based upon the Fe^{3+} located on the *C*-site. The remaining cations were fixed on sites according to their ionic radius, i.e., Ca^{2+} on the *X*-site (24*c*), Zr^{4+} on the *Y*-site (16*a*) with Al^{3+} and Si^{4+} located on the *Z*-site (24*d*). Such assignments were in agreement with the traditional location of cations in garnets.

Table 4
Illustrative literature values from Mössbauer spectroscopic analysis of Fe containing garnets, references are shown in brackets. The composition of the Kimzeyite is the same as that outlined in the electron channelling analysis

System	*B*-site (Octahedral)		*C*-site (Tetrahedral)	
	Isomer shift ($mm\,s^{-1}$)	Quadrupole split ($mm\,s^{-1}$)	Isomer shift ($mm\,s^{-1}$)	Quadrupole split ($mm\,s^{-1}$)
$Y_3Fe_5O_{12}$ [11]	0.38	0.47	0.16	0.97
$YCa_2Zr_2Fe_2AlO_{12}$ [11]	—	—	0.17	1.09
$Ca_3Fe_2Si_3O_{12}$ [11]	0.41	0.59	—	—
$Ca_3Fe_2Ti_{1.42}Si_{1.58}O_{12}$ [14]	0.40	0.75	0.20	1.15
Kimzeyite [12]	0.45	1.01	0.19	1.08

Table 5
Results from Rietveld refinement of recorded neutron diffraction data, positional parameters are shown for the variable O-96*h* position, isothermal parameters for all sites are multipled by 100. Values in brackets are those esd's quoted by GSAS, wR_p and R_p are calculated using the standard equations

	$Ca_3Zr_2FeAlSiO_{12}$	$Ca_3Zr_2Fe_{1.5}Al_{0.5}SiO_{12}$	$Ca_3Zr_2Fe_2SiO_{12}$	$Ca_3Hf_2FeAlSiO_{12}$	$Ca_3Hf_2Fe_2SiO_{12}$
Unit cell–a/Å	12.5122(18)	12.5844(7)	12.6164(6)	12.5145(7)	12.5898(6)
Ca (24c)–U_{iso}	0.70(16)	0.63(9)	0.83(8)	0.96(9)	0.85(9)
Zr/Hf (16a)–U_{iso}	0.52(11)	0.58(6)	0.63(5)	0.45(5)	0.42(5)
Al/Fe/Si (24d)–U_{iso}	1.07(15)	0.51(7)	0.57(6)	0.56(7)	0.63(6)
O 96h_x	−0.03445(15)	−0.03362(11)	−0.03318(11)	−0.03452(11)	−0.03312(11)
O 96h_y	0.05101(15)	0.05142(12)	0.05152(11)	0.05045(11)	0.05113(12)
O 96h_z	0.15499(18)	0.15450(13)	0.15365(12)	0.15437(11)	0.15357(12)
O U_{iso}	1.03(10)	1.04(5)	1.27(5)	1.15(5)	1.33(5)
wR_p	0.0461	0.0528	0.0504	0.0486	0.0479
R_p	0.0315	0.0380	0.0379	0.0360	0.0352

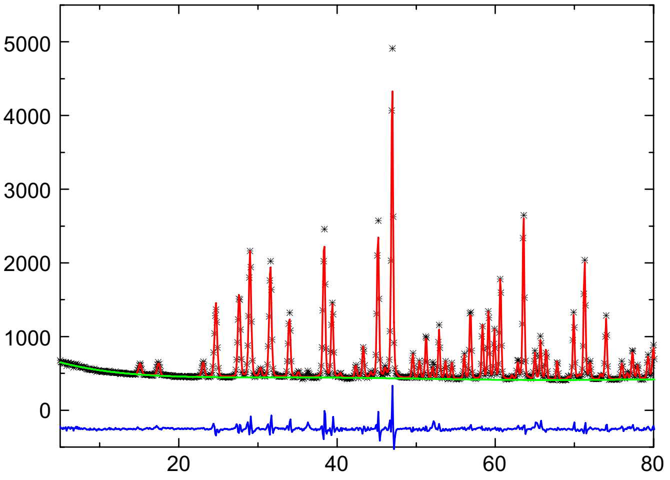

Fig. 4. Graphical results from the refinement of $Ca_3Zr_2FeAlSiO_{12}$, the crosses are the recorded data, the solid line the model refined, the vertical ticks indicate the reflection locations, and the bottom line the difference between model and data. The intensities at ~37° and ~42° are due to an unknown source, but were visible in all samples, collected at the same time.

The change in unit-cell is linearly related to the change in the average *Z*-site ionic radius or the O-*96h* position; they are linked with each other, and as such agree with Vegard's law. Such an observation is to be expected as the only substantial change across both series is the *Z*-site composition, which in turn is linked to the O-*96h* position.

3.5. Bond valence analysis

Bond valence analysis is routinely used for analysing bond lengths within in a refined structure to help confirm the accuracy of the refinement. Using the equation published by Brese and O'Keefe [16] the values for S_{ij} were calculated and are included in Table 6, the values used for S_o are from Brese and O'Keefe [16]. The values for S_{ij} are in reasonable agreement with those expected e.g., Ca on the *X*-site would be 2.00. The average valence for the *Z* site in these samples is expected to be ~3.333, this is due to the site having 0.667 contribution from the Fe^{3+} and Al^{3+} cations and 0.333 contribution from Si^{4+}. The small discrepancies are probably due to inaccuracies in the compositional analysis. These inaccuracies would be scaled during the Rietveld refinement, exact amount dependent on the scattering parameters of the element, thus increasing their impact on the S_{ij} summation. The main error to the calculated S_{ij} would be from any slight misrefinement of the oxygen position, especially as this is the only position that is not fixed and impacts on all cation–anion bonds. Due to the nature of the structure being built of three types of polyhedra, it is possible that the smallest polyhedra can be distorted away from the ideal distance, i.e., to give an average bond valence summation of 3.333. Such a distortion can give rise to the summations for the *Z*-site to differ from the expected value.

Table 6
Bond valence summations, for the first cation-anion shell, using bond lengths calculated from the Rietveld refinement of collected neutron data

System	Bond	CN	Length	Error	S_{ij}	Error
$Ca_3Zr_2FeAlSiO_{12}$	Ca–O	4	2.4085	0.002	2.030	0.011
		4	2.5546	0.0019		
	Zr–O	6	2.0866	0.0023	4.005	0.025
	Al/Fe/Si	4	1.7619	0.002	3.107	0.015
$Ca_3Zr_2Fe_{1.5}Al_{0.5}SiO_{12}$	Ca–O	4	2.4181	0.0014	1.984	0.008
		4	2.5617	0.0015		
	Zr–O	6	2.0924	0.0016	3.942	0.017
	Al/Fe/Si	4	1.7848	0.0015	2.934	0.010
$Ca_3Zr_2Fe_2SiO_{12}$	Ca–O	4	2.4255	0.0014	1.954	0.007
		4	2.5645	0.0014		
	Zr–O	6	2.087	0.0015	4.000	0.016
	Fe/Si	4	1.8006	0.0014	3.210	0.009
$Ca_3Hf_2FeAlSiO_{12}$	Ca–O	4	2.4117	0.0013	2.006	0.007
		4	2.5609	0.0014		
	Hf–O	6	2.0778	0.0015	3.949	0.016
	Al/Fe/Si	4	1.7644	0.0014	3.208	0.011
$Ca_3Hf_2Fe_2SiO_{12}$	Ca–O	4	2.419	0.0014	1.977	0.008
		4	2.5636	0.0015		
	Hf–O	6	2.08	0.0015	3.925	0.016
	Fe/Si	4	1.7692	0.0015	3.495	0.011

In the main however the values are indicative of an accurate refinement of the experimental data.

4. Conclusion

Synthetic samples based upon Kimzeyite have been characterised and found to adopt the garnet structure with unit cell parameters close to others of similar composition. Electron channelling has been used to show that the assignment of cation location of the synthetic samples agree with the naturally occurring kimzeyite mineral. The Mössbauer data has shown that the Fe is located as Fe^{3+} on the tetrahedrally co-ordinated Z site, with no evidence of distribution onto either the X or Y sites, or evidence of magnetic ordering. The change in unit cell size has been found to be related to the change in the Z site composition and is in agreement with Vegard's law. The synthesis of new garnets containing Hf which have very similar structural properties to Zr containing ones allows a new suite of samples to be synthesised that can be used to study chemical and radioactive stability.

Acknowledgments

We would like to acknowledge funding by CMI , the Cambridge-MIT Institute, Nexia Solutions and the EPSRC (EP/C510259/1). The authors would also like to acknowledge Drs. Swainson and Cranswick at the Chalk River laboratories for their expert help in the collection and analysis of the neutron diffraction data.

References

[1] G.A. Novak, G.V. Gibbs, Am. Mineral. 56 (1971) 791.
[2] L. Lupini, C.T. Williams, A.R. Woolley, Mineral. Mag. 56 (1992) 581.
[3] C. Milton, B.L. Ingram, L.V. Blade, Am. Mineral. 46 (1961) 533.
[4] R. Munno, G. Rossi, C. Tadini, Am. Mineral. 65 (1980) 188.
[5] E. Schingaro, F. Scordari, F. Capitanio, G. Parodi, D.C. Smith, A. Mottana, Eur. J. Mineral. 13 (2001) 749.
[6] G.R. Lumpkin, K.L. Smith, M.G. Blackford, R. Giere, C.T. Williams, Micron 25 (1994) 581.
[7] C.J. Rossouw, P.S. Turner, T.J. White, A.J. O'Connor, Philos. Mag. Lett. 60 (1989) 225.
[8] P.S. Turner, T.J. White, A.J. O'Connor, C.J. Rossouw, J. Microsc. 162 (1991) 369.
[9] A.C. Larson, R.B. Von Dreele, General Structure Analysis System (GSAS), Los Alamos National Laboratory Report LAUR, 2000.
[10] B.H. Toby, J. Appl. Crystallogr. 34 (2001) 210.
[11] F.J. Berry, J.Z. Davalos, J.R. Gancedo, C. Greaves, J.F. Marco, P. Slater, M. Vithal, J. Solid State Chem. 122 (1996) 118.
[12] E. Dowty, Am. Mineral. 56 (1971) 1983.
[13] F.E. Huggins, D. Virgo, H.G. Huckenholz, Am. Mineral. 62 (1977) 475.
[14] F.E. Huggins, D. Virgo, H.G. Huckenholz, Am. Mineral. 62 (1977) 646.
[15] J. Ito, C. Frondel, Am. Mineral. 52 (1967) 773.
[16] N.E. Brese, M. O'Keeffe, Acta Crystall. B—Struct Sci B 47 (1991) 192.